

Polymer Dispersity Control via Organocatalyzed Living Radical Polymerization

Xu Liu, Chen-Gang Wang, and Atsushi Goto*

Abstract: Molecular weight distribution of polymer, termed dispersity (\mathcal{D}), is a fundamental key parameter for determining polymer material properties. This paper reports a novel approach for controlling \mathcal{D} , exploiting a temperature-selective radical generation in organocatalyzed living radical polymerization. The polymers with tailored \mathcal{D} were synthesized in a batch system without the assistance of an external pump. A unique aspect of this approach is that \mathcal{D} was tuneable from 1.11 to 1.50 in any segments in diblock, triblock, and multi-block copolymers and any forms of star and brush polymers without segmental or topological restriction. This approach is amenable to various monomers and free from metals, which are attractive for applications. The approach was also able to generate polymer brushes on surfaces with tailored \mathcal{D} . An interesting finding was that the polymer brushes exhibited unique interaction with external molecules, depending on \mathcal{D} .

Molecular weight distribution of polymer, termed dispersity ($\mathcal{D} = M_w/M_n$), is a fundamental key parameter to determine the polymer properties such as processability, viscoelasticity, and self-assembly behaviors, where M_w and M_n are the weight- and number-average molecular weights, respectively.^[1–6] Living radical polymerization (LRP) facilitates the synthesis of polymers with small \mathcal{D} as well as pre-determined molecular weights and sophisticated architectures.^[7–12] However, polymers with large \mathcal{D} are occasionally desired for improved physical properties such as miscibility and processability, and the manipulation of \mathcal{D} in LRP is an important topic but is still challenging.

Several approaches have been developed to manipulate \mathcal{D} . Blending polymers with different molecular weights is often applied.^[13–15] The polymers need to be prepared in multiple independent runs, and the blended polymers often have multimodal molecular weight distribution. By optimizing the polymerization conditions such as catalyst loadings, initiators, temperatures and additional chain transfer agents, \mathcal{D} was modulated at 1.1–2.0 in LRP.^[16–18] However, the attained large \mathcal{D} usually arose from inefficient control in LRP. Thus, the obtained polymers hardly undergo further chain extension. Recently, Fors et al. elegantly varied \mathcal{D} and molecular weight distribution “shapes” by metering the addition of an initiator using a feeding pump in anionic and nitroxide-mediated polymerizations.^[19–22] This approach was applied to homopolymers and the first segment of block copolymers but not to the other segments of block copolymers. Boyer et al. recently metered the addition of polymeric initiator (macroinitiator) in a photo-controlled LRP and successfully obtained block copolymers with tailored \mathcal{D} in the second segment.^[23,24] However, the pump-assisted method is always inapplicable to heterogeneous systems such as polymer

brush synthesis from solid substrates, which limits applications.

We have developed an organocatalyzed LRP, i.e., reversible complexation mediated polymerization (RCMP) that uses alkyl iodides (R–I) as dormant species and organic catalysts such as $\text{Bu}_4\text{N}^+\text{I}^-$ (BNI) (Scheme S1 in Supporting Information).^[25–28] In RCMP, iodide anion I^- (catalyst) coordinates R–I (dormant species) to form an R–I \cdots I $^-$ complex via halogen bonding, which is followed by the R–I bond cleavage to generate a propagating radical R^\bullet . The rate of the generation of R^\bullet depends on the R group.^[29] The R–I bond for R = acrylate polymer (with a secondary alkyl chain end) is significantly stronger than that for R = methacrylate polymer (with a tertiary alkyl chain end). Therefore, an elevated temperature (e.g., 110 °C) is required for the acrylate polymerizations, while a mild temperature (e.g., 60–70 °C) is sufficient for the methacrylate polymerizations.^[29] We previously exploited this temperature selectivity to synthesize multi-block copolymers and nano-particles.^[30]

In the present study, we newly applied this temperature selectivity to develop a novel method to modulated \mathcal{D} without the assistance of pumps. The method is to utilize a small amount of butyl acrylate (BA) in an RCMP of methyl methacrylate (MMA) at a mild temperature. Once a propagating radical possesses BA at the terminal unit and is then capped with iodide, the generated polymer-iodide hardly re-initiates at the mild temperature.^[29] The BA-terminal dormant species gradually accumulate in the course of polymerization, increasing \mathcal{D} (Figure 1a). The amount of the accumulated BA-terminal dormant species (and hence \mathcal{D}) can be modulated by the amount of BA.

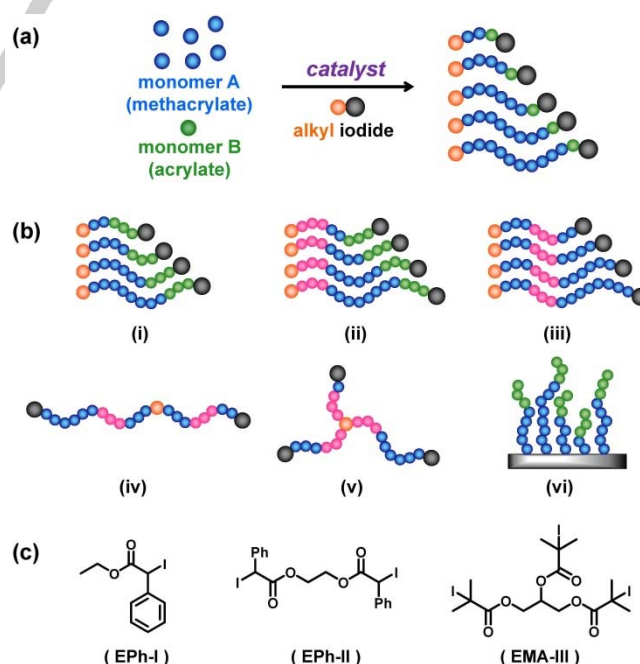


Figure 1. (a) Synthesis of polymer with high dispersity and high iodide chain-end fidelity. (b) Applications to various types of block copolymers. (c) Alkyl iodide initiators used in this work.

Dr. X. Liu, Dr. C-G. Wang, Prof. Dr. A. Goto
Institution Division of Chemistry and Biological Chemistry, School of
Physical and Mathematical Sciences, Nanyang Technological University,
21 Nanyang Link, 637371 Singapore
E-mail: agoto@ntu.edu.sg

Importantly, the BA-terminal dormant species are not “dead” polymers but can still re-initiate at high temperatures to yield block copolymers (Figure 1b). This method is able to modulate \mathcal{D} in any segments in diblock, triblock, and multi-block copolymers and any forms of branched polymers without segmental or topological restriction. Because of the pump-free nature, this approach can have access to even heterogeneous systems. An example described below is the synthesis of polymer brushes with tailored \mathcal{D} , which is unique to this approach. An interesting finding was that the polymer brush exhibited a \mathcal{D} -dependent size-exclusion property to an external molecule.

We heated a mixture of monomer (8000 mM, MMA and BA), an initiating dormant species (EPh-I (Figure 1c), 80 mM), and a catalyst (BNI, 80 mM) at a mild temperature of 70 °C. MMA was a main monomer, and BA was a co-monomer. We varied the [MMA]/[BA] ratio from 100/0 to 90/10. Figure 2 (open circles) and Table 1 (entry 1) shows the 100/0 system (homopolymerization of MMA). The polymerization proceeded up to a 78% monomer conversion for 4 h. The M_n agreed with the theoretical value ($M_{n,theo}$), and \mathcal{D} was low (1.13–1.19) throughout the polymerization.

In contrast, the 90/10 (MMA/BA) system (Figure 2 (filled circles) and Table 1 (entry 4)) resulted in a significant increase in \mathcal{D} (1.16–1.45), keeping good agreement of M_n with $M_{n,theo}$. The growing chain end turned to the BA-terminal iodide gradually, leading to a slowdown of the polymerization and an increase in \mathcal{D} . The monomer conversion reached a plateau (59%) after 14 h, indicating a full BA-terminal dormancy. The BA-terminal fraction (F) was determined with ^1H NMR (Figure 3a) from the peak areas for the initiating C_6H_5 moiety (7.23–7.39 ppm) and CH of the terminal BA unit (4.39–4.48 ppm).^[31] The F value reached 95% (with $\pm 5\%$ experimental error) after 14 h, quantitatively confirming the full BA-terminal dormancy.

The ^1H NMR (Figure 3a) shows that the polymer obtained at 14 h possesses 67 MMA units and 4 BA units on average. The BA units were more than 1, because the generated PMMA with a terminal BA radical (PMMA-BA*) could react with MMA for further propagation or be capped with iodide (Figure 3b), where PMMA is poly(methyl methacrylate). The chain growth stops only when PMMA-BA* is capped with iodide. The further propagating chain continues to grow until it reacts with BA and is capped with iodide. Therefore, 4 BA units were consumed for the full BA-terminal dormancy, yielding a random copolymer of MMA (67 units) and BA (3 units) with 1 terminal BA unit. Although the copolymer nature is a deviation from the ideal homopolymer of MMA, such a minimal amount (only 4 units) of BA required is highly attractive for practical use. The addition of I_2 (deactivator in RCMP) (Table 1, entry 5) enabled an increased rate of the iodide capping and effectively decreased the required BA units to 2. However, this was achieved at the expense of a narrower tunable window of \mathcal{D} (1.13–1.33) and a slower polymerization.

A reduced amount of BA from [MMA]/[BA] = 90/10 to 95/5 (Figure 2 (triangles) and Table 1 (entry 3)) still provided a similar tuneable window (\mathcal{D} up to 1.44), while the BA-terminal dormancy was not quantitative ($F = 74\%$). A further reduced amount of BA to [MMA]/[BA] = 98/2 (Figure 2 (squares) and Table 1 (entry 2)) resulted in a narrower tuneable window (\mathcal{D} up to 1.26) and a lower BA-terminal dormancy ($F = 29\%$).

It is worth noting that both of the BA- and MMA-terminal polymers can serve as macro-initiators and re-initiate at an elevated temperature to give block copolymers (see below). The initiation efficiency for BA- and MMA-terminal dormant species are sufficiently high to attain virtually uniform initiation.^[29] A full BA-terminal dormancy is ideal but unessential for the subsequent block polymerization. Therefore, the obtained polymers at arbitrary time could be used as macroinitiators in the subsequent polymerization.

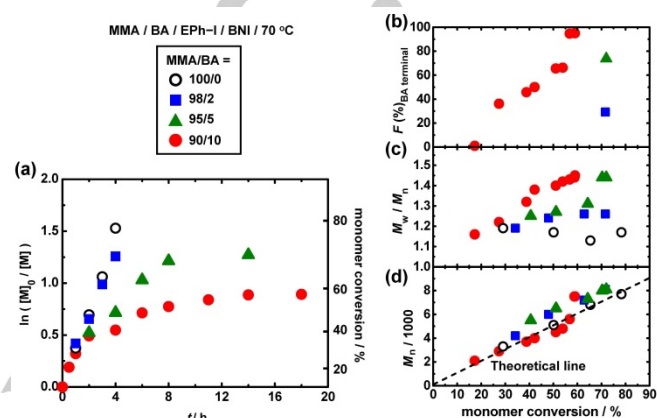


Figure 2. Plots of (a) $\ln([M]_0/[M])$ vs t and (b, c, and d) fraction of BA terminal chain, M_w/M_n , and M_n vs monomer conversion for the MMA/BA/EPh-I/BNI systems (70 °C); [monomers] $_0$ = 8000 mM; [EPh-I] $_0$ = 80 mM; [BNI] $_0$ = 80 mM. The MMA/BA ratios and symbols are indicated in the figure. The F value in (b) was determined for only the longest polymerization time for the [MMA] $_0$ /[BA] $_0$ = 98/2 and 95/5 systems.

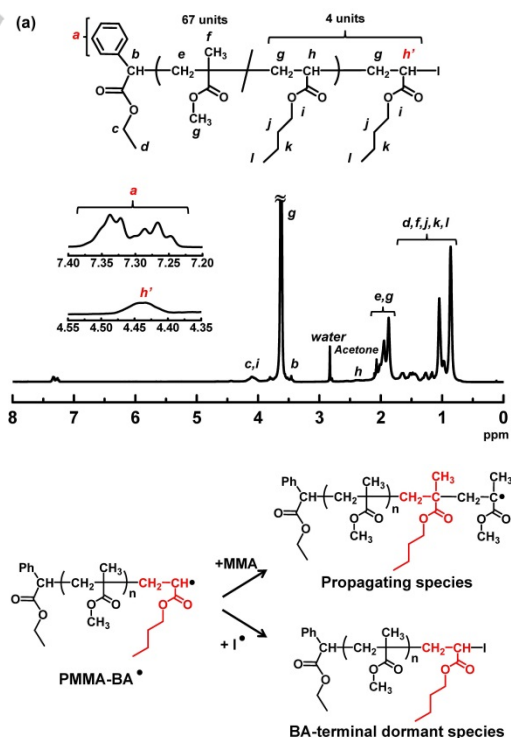


Figure 3. (a) ^1H NMR spectrum (acetone- d_6) of the obtained PMMA-I (Table 1, entry 4). (b) Reaction of PMMA-BA* with MMA and I*.

Table 1. Polymerizations of methacrylates in the presence of BA.

Entry	monomer	[monomer] ₀ /[BA] ₀ /[EPH-I] ₀ /[BNI] ₀ (mM)	T (°C)	t (h)	conv (%) ^[a]	$M_n^{[b]}$ ($M_{n,theo}^{[c]}$)	$\mathcal{D}^{[b]}$	Range of $\mathcal{D}^{[d]}$
1	MMA	8000/0/80/80(100/0/1/1)	70	4	78	7700(8100)	1.17	1.13–1.19
2	MMA	7840/160/80/80(98/2/1/1)	70	4	72	8100(7500)	1.26	1.19–1.26
3	MMA	7600/400/80/80(95/5/1/1)	70	14	72	8100(7200)	1.44	1.25–1.44
4	MMA	7200/800/80/80(90/10/1/1)	70	18	59	7500(6100)	1.45	1.16–1.45
5	MMA	7200/800/80/80(90/10/1/1) ^[e]	70	18	40	4800 (4200)	1.33	1.11–1.33
6	MMA	7730/270/27/27(290/10/1/1)	70	18	48	19000(14000)	1.43	1.20–1.43
7	MMA	7840/160/16/16(490/10/1/1)	70	18	44	25000(22000)	1.43	1.16–1.43
8	MMA	7900/100/10/10(790/10/1/1)	70	18	44	40000(35000)	1.40	1.12–1.40
9	BzMA ^[f]	7200/800/80/80(90/10/1/1)	70	18	53	9800(8800)	1.46	1.20–1.46
10	GMA ^[f]	7200/800/80/80(90/10/1/1)	60	2	59	9100(8000)	1.44	1.25–1.44
11	DMAEMA ^[f]	7200/800/80/80(90/10/1/1)	70	4	37	6600(5700)	1.39	1.10–1.39

[a] Monomer conversion. [b] PMMA-calibrated GPC values. [c] Theoretical M_n calculated with [monomer]₀, [BA]₀, [EPH-I]₀, and monomer conversion. [d] A tunable window of \mathcal{D} . [e] The addition of I_2 (8 mM). [f] BzMA = benzyl methacrylate, GMA = glycidyl methacrylate, and DMAEMA = 2-(dimethylamino)ethyl methacrylate.

This method was applicable to higher molecular weights. The targeted degree of polymerization (DP) at a full (100%) monomer conversion increased to 300, 500 and 800 (Table 1 (entries 6–8) and Figure S2). A higher target DP results in a lower BA composition in the polymer at the fixed amount of BA. The polymer becomes even closer to a homopolymer of MMA.

The monomer scope was wide. Besides MMA, the amenable main monomers included functional methacrylates with benzyl (BzMA), glycidyl (GMA), and dimethyl amino (DMAEMA) groups with tuned \mathcal{D} (1.10–1.46) (Table 1 (entries 9–11)). For the comonomer, not only an acrylate (BA) but also other families of monomer, i.e., vinyl acetate, *N,N*-dimethyl-acrylamide, *N*-vinyl-2-pyrrolidone, and ethyl vinyl ketone, were successfully utilized (\mathcal{D} = 1.15–1.60) (Table S1).

The BA-terminal polymer, which is dormant at 70 °C, was able to re-initiate at a high temperature 110 °C and yielded block copolymers. At 110 °C, a PMMA-I macro-initiator (M_n = 7500, \mathcal{D} = 1.45, and F = 95% (Table 1 (entry 4)) successfully initiated the polymerizations of hydrophobic, biocompatible, amphiphilic, and functional acrylates (Figure 4a–e and Table S2), yielding block copolymers (M_n = 9400–11000 and \mathcal{D} = 1.17–1.27). The \mathcal{D} values of the block copolymers (1.17–1.27) were smaller than that of the macro-initiator (1.45), meaning that the second blocks have low \mathcal{D} values. The GPC chromatograms (Figure 4a–e) show that a large fraction of the macro-initiator chains smoothly extended to the block copolymers, suggesting high block efficiency.

This method enabled the modulation of \mathcal{D} in not only the first block segment (as demonstrated above) but also the second and third segments in block copolymers. A low-dispersity PBzMA-I (M_n = 6200 and \mathcal{D} = 1.15) was prepared as the first block segment, and the subsequent polymerization of MMA with a small amount of BA (MMA/BA = 90/10) successfully yielded PBzMA-*b*-PMMA diblock copolymers with tuned \mathcal{D} (1.24–1.42), where PBzMA is poly(benzyl methacrylate) (Figure 4f and Table S3 (entry 1)). The \mathcal{D} values (1.24–1.42) were larger than that of the macro-initiator (1.15), meaning the efficient modulation of \mathcal{D}

in the second block. The obtained diblock copolymer (M_n = 16000 and \mathcal{D} = 1.42) was further used as a macro-initiator to generate a PBzMA-*b*-PMMA-*b*-PBA (ABC) triblock copolymer (M_n = 20000 and \mathcal{D} = 1.33), where PBA is poly(butyl acrylate). The \mathcal{D} value of the triblock copolymer (1.33) was smaller than that of the diblock macro-initiator (1.42), meaning that the third block has a low \mathcal{D} value. Similarly, \mathcal{D} was tuned in the third block in PMMA-*b*-PBzMA-*b*-PMMA triblock copolymers (\mathcal{D} = 1.17–1.50), which were synthesized from a low-dispersity PMMA-*b*-PBzMA (M_n = 6200 and \mathcal{D} = 1.11) diblock copolymer (Figure 4g and Table S3 (entry 2)).

Instead of an alkyl mono-iodide (EPH-I) used above, we employed alkyl di-iodide (EPH-II) and tri-iodide (EMA-III) initiators (Figure 1c) and prepared ABABA multi-block copolymers and 3-arm star block copolymers, respectively. We obtained PMMA-*b*-PBzMA-*b*-PMMA-*b*-PBzMA-*b*-PMMA multi-block copolymers with tuned \mathcal{D} in the third blocks (two PMMA end segments) (\mathcal{D} = 1.16–1.40) (Figure 4h and Table S3 (entry 3)) and BzMA-*b*-PMMA-III star-shaped-block copolymers with tuned \mathcal{D} in the second blocks (three PMMA end segments) (\mathcal{D} = 1.26–1.49) (Figure 4i and Table S3 (entry 4)). These results clearly demonstrate sequential and topological versatility of this approach, enabling the access to tailored \mathcal{D} in any segments in linear and branched block copolymers.

A unique application described here is the synthesis of polymer brushes with tailored \mathcal{D} , to which the pump-assisted method is not applicable. Surface-initiated living radical polymerization is an emerging technique to yield concentrated polymer brushes with low \mathcal{D} , which exhibit unique properties such as ultra-low friction and super-antifouling.^[32–35] However, concentrated polymer brushes with high \mathcal{D} are unexplored and may exhibit new functions.

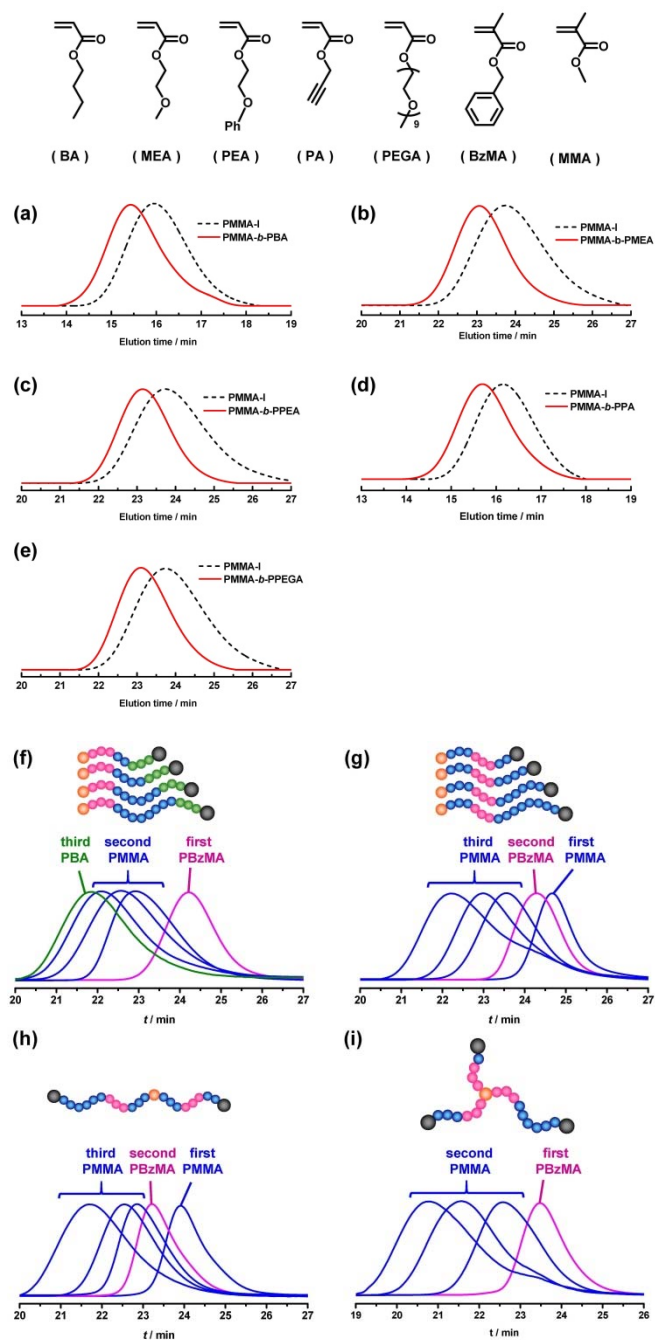


Figure 4. GPC traces for the synthesis of block copolymers. The reaction conditions are given in Tables S2 and S3.

A surface-immobilizing alkyl iodide initiator (6-(2-iodo-2-isobutyloxy)hexyltriethoxysilane) was attached on a silicon wafer. The wafer was immersed in a mixture of MMA, a non-immobilized free initiator EPh-I, and a catalyst BNI in the presence and absence of BA at 70 °C, yielding concentrated polymer brushes with a high \bar{D} value of 1.50 (brush **A**) and a low \bar{D} value of 1.13 (brush **B**), respectively, with keeping similar M_n values (29000 (brush **A**) and 35000 (brush **B**)) (Table S4 (step 1)). Because the \bar{D} and M_n values of the free polymer obtained

from the free initiator are generally in good agreement with those of the brush polymers,^[32] we measured the \bar{D} and M_n values of the free polymers and assumed the identical values for the brush polymers.

The obtained graft and free polymers were subsequently used as macro-initiators for the block polymerization of propargyl acrylate (PA) at 110 °C (Table S4 (step 2)). A short second block was intentionally targeted for the following experiment. The M_n increased from 29000 to 31000 for brush **A** and 35000 to 37000 for brush **B**, showing successful chain extension. The \bar{D} value virtually remained unchanged (1.50 to 1.53 and 1.13 to 1.12, respectively), because of the short second block. The surface occupancy (σ^*) was similarly high for the two brushes (19% (brush **A**) and 22% (brush **B**)) and located in the concentrated brush region ($\sigma^* > 10\%$).^[32]

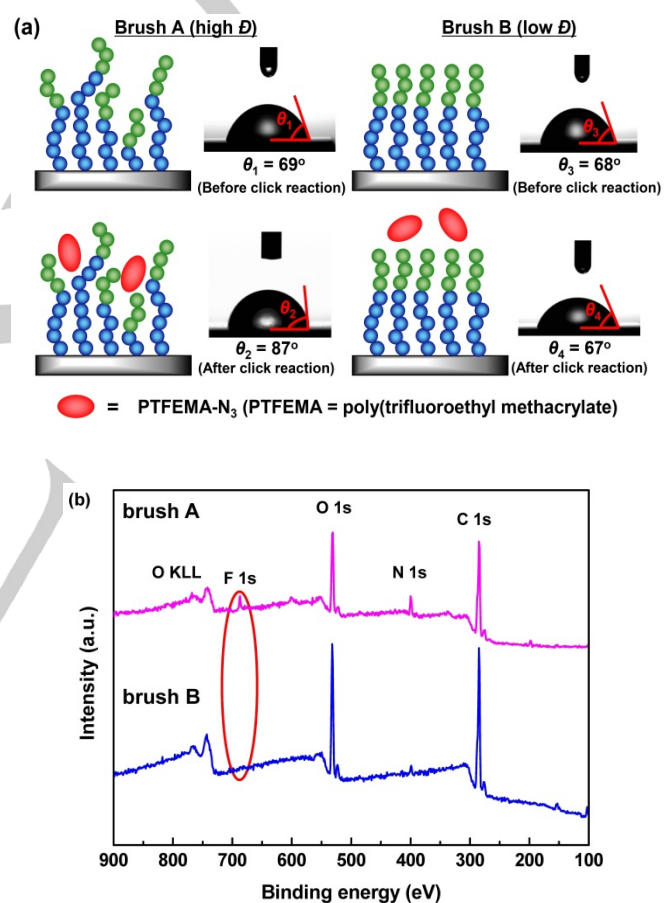


Figure 5. (a) Different size exclusion effects to external solute molecules for polymer brushes with high \bar{D} (brush **A**) and low \bar{D} (brush **B**). Water contact angle (θ) of PMMA-b-PPA brushes **A** and **B** before and after the click reaction with PTFEMA- N_3 . (b) XPS survey spectra of brushes **A** and **B** after the click reaction with PTFEMA- N_3 .

We observed a unique size exclusion effect from the two brushes. We synthesized a low-dispersity poly(trifluoroethyl methacrylate) bearing an azide at a chain end (PTFEMA- N_3 , M_n = 9900, \bar{D} = 1.12). We studied a copper-catalyzed azide-alkyne cycloaddition of PTFEMA- N_3 with the two brushes (brushes **A**

and **B**). PTFEMA-N₃ may attach to the alkyne groups (in the PA block) in the brushes.

Concentrated polymer brush chains with low \bar{D} (brush **B**) are highly stretched because of the steric hindrance of the neighboring chains (Figure 5a), preventing large-size solute molecules from diffusing into the brush layer (size exclusion). Because of the low \bar{D} , the chains are uniform in length and stretch to the outermost surface, giving a low molecular weight (10^2 – 10^3) size exclusion limit with high resolution.^[32] In sharp contrast, concentrated brush chains with high \bar{D} (brush **A**) are not uniform in length and hence flexible in their conformation despite the high graft densities, allowing even large solute molecules to diffuse into the brush layer. This would give a high molecular weight ($>10^3$) size exclusion limit.

The studied solute (PTFEMA-N₃) was a large molecule (molecular weight $\sim 10^4$). Brush **B** with low \bar{D} completely excluded PTFEMA-N₃, resulting in no attachment of PTFEMA-N₃ on the brush, as we observed no change in the surface contact angle (θ) before and after the click reaction (68° and 67°, respectively (water droplet)) (Figure 5a). In contrast, brush **A** with high \bar{D} allowed PTFEMA-N₃ to diffuse into the brush layer, resulting in the linkage of PTFEMA-N₃ to the brush. The θ value significantly increased from 69° to 87° because of the hydrophobicity of the fluorinated PTFEMA. This size-exclusion experiment was carried out three times, confirming the reproducibility (Figure S3).

The surfaces after the click reaction were also analyzed with X-ray photoelectron spectroscopy (XPS) (Figure 5b). Brush **A** with high \bar{D} showed a strong fluorine signal because of the attachment of PTFEMA (F/O ratio = 12/100), while brush **B** with low \bar{D} showed only a very weak fluorine signal (F/O ratio = 0.96/100). The significant differences in the contact angles and XPS fluorine intensity between the two brushes clearly demonstrate the unique size exclusion to external molecules.

In conclusion, a novel and pump-free approach for tailoring \bar{D} was successfully developed based on a temperature-selective activation of the dormant species in RCMP. The use of small amounts of co-monomer, the amenability to various main monomers (functional methacrylates), and the metal-free nature are attractive in extensive use. The \bar{D} value is tunable in any segments of linear and branched block copolymers without segmental or topological restriction. This method is also applicable to heterogeneous systems such as polymer brush synthesis. The observed unique \bar{D} -dependent size exclusion effect of the polymer brush may open up novel functional interfaces for biological and sensing applications.

Acknowledgements

This work was supported by Academic Research Fund (AcRF) Tier 2 from Ministry of Education in Singapore (MOE2017-T2-1-018).

Keywords: polymerizations • block copolymers • polymer dispersity • temperature selectivity • polymer brush

- [1] N. A. Lynd, A. J. Meuler, M. A. Hillmyer, *Prog. Polym. Sci.* **2008**, *33*, 875–893.
- [2] K. E. B. Doncom, L. D. Blackman, D. B. Wright, M. I. Gibson, R. K. O'Reilly, *Chem. Soc. Rev.* **2017**, *46*, 4119–4134.
- [3] R. B. Grubbs, R. H. Grubbs, *Macromolecules* **2017**, *50*, 6979–6997.
- [4] J. M. Widin, A. K. Schmitt, A. L. Schmitt, K. Im, M. K. Mahanthappa, *J. Am. Chem. Soc.* **2012**, *134*, 3834–3844.
- [5] A. K. Schmitt, M. K. Mahanthappa, *Macromolecules* **2014**, *47*, 4346–4356.
- [6] J. Aho, J. P. Boetker, S. Baldursdottir, J. Rantanen, *Int. J. Pharm.* **2015**, *494*, 623–642.
- [7] J. Nicolas, Y. Guillauneuf, C. Lefay, D. Bertin, D. Gigmès, B. Charleux, *Prog. Polym. Sci.* **2013**, *38*, 63–235.
- [8] K. Matyjaszewski, N. V. Tsarevsky, *J. Am. Chem. Soc.* **2014**, *136*, 6513–6533.
- [9] M. R. Hill, R. N. Carmean, B. S. Sumerlin, *Macromolecules* **2015**, *48*, 5459–5469.
- [10] D. J. Keddie, G. Moad, E. Rizzardo, S. H. Thang, *Macromolecules* **2012**, *45*, 5321–5342.
- [11] C. Boyer, N. A. Corrigan, K. Jung, D. Nguyen, T.-K. Nguyen, N. N. M. Adnan, S. Oliver, S. Shanmugam, J. Yeow, *Chem. Rev.* **2016**, *116*, 1803–1949.
- [12] K. Matyjaszewski, *Adv. Mater.* **2018**, *30*, 1706441.
- [13] Y. Aoki, L. Li, H. Uchida, M. Kakiuchi, *Macromolecules* **1998**, *31*, 7472–7478.
- [14] X. Ye, T. Sridhar, *Macromolecules* **2005**, *38*, 3442–3449.
- [15] D. Roy, C. B. Giller, T. E. Hogan, C. M. Roland, *Polymer* **2015**, *81*, 111–118.
- [16] J. Listak, W. Jakubowski, L. Mueller, A. Plichta, K. Matyjaszewski, M. R. Bockstaller, *Macromolecules* **2008**, *41*, 5919–5927.
- [17] A. Plichta, M. Zhong, W. Li, A. M. Elsen, K. Matyjaszewski, *Macromol. Chem. Phys.* **2012**, *213*, 2656–2668.
- [18] V. Yadav, N. Hashmi, W. Ding, T.-H. Li, M. K. Mahanthappa, J. C. Conrad, M. L. Robertson, *Polym. Chem.* **2018**, *92*, 4332–4342.
- [19] V. Kottisch, D. T. Gentekos, B. P. Fors, *ACS Macro Lett.* **2016**, *5*, 796–800.
- [20] D. T. Gentekos, L. N. Dupuis, B. P. Fors, *J. Am. Chem. Soc.* **2016**, *138*, 1848–1851.
- [21] D. T. Gentekos, J. Jia, E. S. Tirado, K. P. Barteau, D.-M. Smailgies, R. A. DiStasio, B. P. Fors, *J. Am. Chem. Soc.* **2018**, *140*, 4639–4648.
- [22] D. T. Gentekos, B. P. Fors, *ACS Macro Lett.* **2018**, *7*, 677–682.
- [23] N. Corrigan, A. Almasri, W. Taillades, J. Xu, C. Boyer, *Macromolecules* **2017**, *50*, 8438–8448.
- [24] N. Corrigan, R. Manahan, Z. T. Lew, J. Yeow, J. Xu, C. Boyer, *Macromolecules* **2018**, *51*, 4553–4563.
- [25] A. Goto, T. Suzuki, H. Ohfujii, M. Tanishima, T. Fukuda, Y. Tsujii, H. Kaji, *Macromolecules* **2011**, *44*, 8709–8715.
- [26] A. Goto, A. Ohtsuki, H. Ohfujii, M. Tanishima, H. Kaji, *J. Am. Chem. Soc.* **2013**, *135*, 11131–11139.
- [27] A. Ohtsuki, L. Lei, M. Tanishima, A. Goto, H. Kaji, *J. Am. Chem. Soc.* **2015**, *137*, 5610–5617.
- [28] C.-G. Wang, A. Goto, *J. Am. Chem. Soc.* **2017**, *139*, 10551–10560.
- [29] L. Lei, M. Tanishima, A. Goto, A. H. Kaji, Y. Yamaguchi, H. Komatsu, T. Jitsukawa, M. Miyamoto, *Macromolecules* **2014**, *47*, 6610–6618.
- [30] J. Zheng, C.-G. Wang, Y. Yamaguchi, M. Miyamoto, A. Goto, *Angew. Chem.* **2018**, *130*, 1568–1572; *Angew. Chem. Int. Ed.* **2018**, *57*, 1552–1556.
- [31] L. Xiao, K. Sakakibara, Y. Tsujii, A. Goto, *Macromolecules* **2017**, *50*, 1882–1891.
- [32] Y. Tsujii, K. Ohno, S. Yamamoto, A. Goto, T. Fukuda, *Adv. Polym. Sci.* **2006**, *197*, 1–45.
- [33] M. Krishnamoorthy, S. Hakobyan, M. Ramstedt, J. E. Gautrot, *Chem. Rev.* **2014**, *114*, 10976–11026.
- [34] J. O. Zoppe, N. C. Ataman, P. Mocny, J. Wang, J. Moraes, H.-A. Klok, *Chem. Rev.* **2017**, *117*, 1105–1318.

- [35] W.-L. Chen, R. Cordero, H. Tran, C. K. Ober, *Macromolecules* **2017**, *50*, 4089–4113.

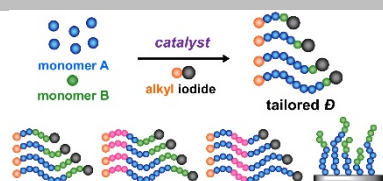
WILEY-VCH

Entry for the Table of Contents (Please choose one layout)

Layout 1:

COMMUNICATION

A novel approach for modulating polymer dispersity was developed. It was based on temperature-selective organocatalyzed living radical polymerization and enabled dispersity modulation in any segments in linear and branched block copolymers and polymer brushes. A dispersity-dependent size-exclusion effect to external molecules was observed on polymer brushes.



*Xu Liu, Chen-Gang Wang, Atsushi Goto**

Page No. – Page No.

Polymer Dispersity Control via Organocatalyzed Living Radical Polymerization